Available online at www.sciencedirect.com
SCIENCE DIRECT®
Scripta Materialia 55 (2006) 57–62
Scripta MATERIALIA
www.actamat-journals.com

Viewpoint Paper

Characterization of three-dimensional crystallographic distributions using polychromatic X-ray microdiffraction

G.E. Ice,* J.W.L. Pang, R.I. Barabash and Y. Puzyrev

Oak Ridge National Laboratory, Metals and Ceramics Division, 1 Bethel Valley Road, Oak Ridge, TN 37831-6118, United States

Received 28 November 2005; revised 24 February 2006; accepted 27 February 2006
Available online 12 April 2006

Abstract—Polychromatic microdiffraction uses small X-ray beams to characterize the local crystallographic structure of materials. When combined with a depth resolving technique called differential aperture microscopy, the phase and local orientation of femtoliter volumes ($0.5 \times 0.5 \times 0.7\ \mu m^3$) can be resolved beneath the surface of a sample. In addition, the local elastic strain and dislocation tensors can also be determined and the local dislocation type can be modeled. Here we present recent technical developments, including example applications and emerging research directions.
© 2006 Acta Materialia Inc. Published by Elsevier Ltd. All rights reserved.

Keywords: X-ray diffraction; Synchrotron radiation; Microdiffraction

1. Introduction

X-ray microdiffraction is a powerful probe of crystal structure with the ability to nondestructively study local structure below the sample surface. However, traditional monochromatic microprobes, are challenged by materials with variations in crystallographic structure; the sample orientation must be precisely adjusted to unknown angles when phase or crystal orientation changes. Other X-ray diffraction approaches, [1,2] allow for rapid measurement of crystal structure distributions, but with limited spatial and/or angular resolution.

The recent development of high-resolution X-ray area detectors, combined with intense X-ray sources now allows polychromatic Laue diffraction on small sample volumes with good spatial and good angular resolution. Combined with advanced nondispersive focusing optics [3] and additional spatially-resolving methods such as differential aperture microscopy [4], it is possible to make unprecedented submicron-resolved measurements of the local three-dimensional (3D) crystal-structure distribution in most materials. In particular, Laue diffraction from small sub-grain volumes detects the local crystal phase, orientation, and deviatoric elastic strain [5]. The 3D local orientation distribution determines the dislocation tensor [4] and the energy of one Laue spot determines the full elastic strain tensor [5].

Formally a Laue pattern from a single crystal is made up of radial line integrals through reciprocal space weighted by the spectral distribution of the incident beam and the structure factor of the sample volume [6]. For example, Figure 1(a) shows a Laue pattern generated by the beamline 34-ID polychromatic microbeam when focused on a $Ni_{80}Fe_{20}$ permalloy single crystal. The small face-centered cubic unit cell of permalloy produces a sparse body-centered cubic Laue pattern that is projected onto the two-dimensional detector. Laue spots include not only fundamental reflections, but may also include weak superstructure reflections arising from short-range order. The weak superstructure reflections can be measured by changing from a polychromatic to a monochromatic beam, with the energy required to probe the superstructure reflections calculated from the polychromatic-determined grain orientation [7].

The formal description of Laue diffraction as a radial line integral is only realized in the ideal case where the X-ray beam impinges on a large single crystal. In real materials, X-rays penetrate through regions with inhomogeneous crystalline structure. Straight-forward Laue diffraction from real materials therefore is typically hard to interpret as it contains the overlapping Laue patterns from thousands of volumes with different crystalline phase, orientation or strain.

* Corresponding author. Tel.: +1 865 574 2744; fax: +1 865 574 7659; e-mail: IceGE@ornl.gv

1359-6462/$ - see front matter © 2006 Acta Materialia Inc. Published by Elsevier Ltd. All rights reserved.
doi:10.1016/j.scriptamat.2006.02.046

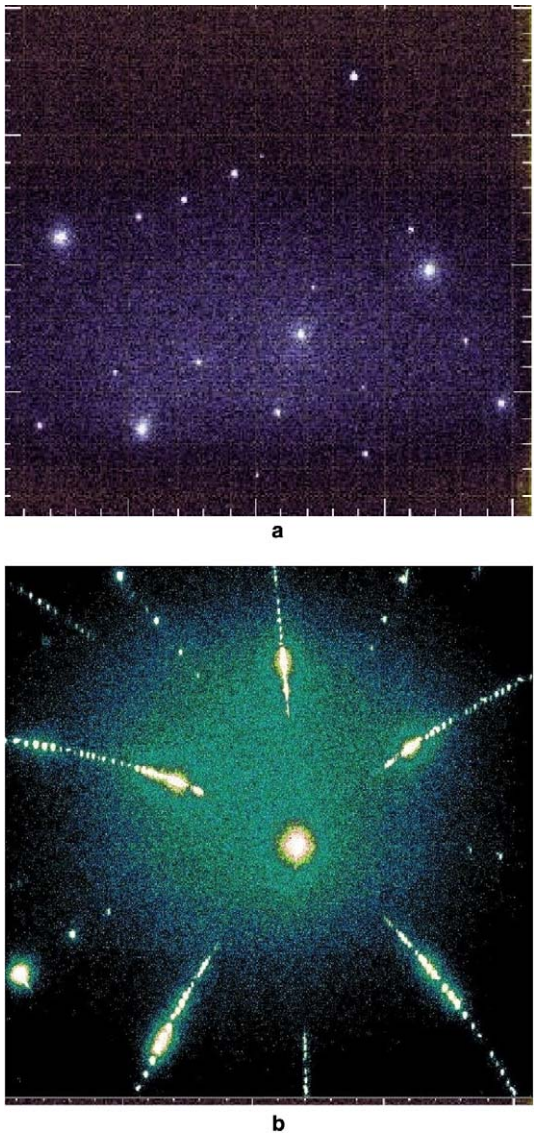

Figure 1. (a) Face-centered cubic permalloy single crytal produces a sparse Laue pattern due to the small unit cell size. (b) GaN single-crystal film on a SiC substrate. The GaN film is crystallograhically aligned with the SiC substrate. The pattern is dominated by the large number of SiC reflections with SiC reflections aligned nearly perfectly in the GaN pattern.

The problem of overlapping Laue patterns is greatly improved by the use of small X-ray beams; small beams restrict the lateral dimensions of the region probed and hence the crystal volume sampled by the beam. However, X-ray beams penetrate microns to millimeters through materials. For example as illustrated in Figure 1(b), the Laue patterns from a thin GaN film and its SiC substrate are superimposed. In this case the atomic registry of the GaN crystal structure to the substrate structure makes the patterns appear to come from a single crystal, although some reflections are from the SiC, some are from the GaN and some are from both SiC and GaN.

For fine-grained low-Z materials the problem of overlapping Laue patterns can be much more complicated than with thin films on single crystal substrates. In fine-grained materials, tens to thousands of distinct grains or subgrains are intercepted by the penetrating X-ray beam. In large deformed crystals the Laue pattern can be modeled [8]. More generally, the signal from diffracting volumes along the penetrating beam can be disentangled by the knife edge technique called differential aperture microscopy (Fig. 2) [4]. Here Laue pattern differences before and after a smooth high-Z wire is translated near the sample can be used to locate the origin of diffracted intensity detected by each pixel of the detector.

The combination of differential aperture microscopy together with polychromatic microdiffraction allows for a wide range of materials to be studied nondestructively with good spatial and with good angular resolution to the local crystallographic orientation and deviatoric strain. To exploit this opportunity, a dedicated instrument dubbed the 3D X-ray crystal microscope has been developed on station 34-ID-E at the Advanced Photon Source [9]. This instrument incorporates advanced nondispersive focusing optics with an insertable, nondispersive monochromator to extend the kinds of experiments that can be performed. A schematic of the key elements of the instrument is given in Figure 3. Below we describe recent experimental programs that illustrate emerging applications of polychromatic microdiffraction to thin-film and bulk materials.

2. Applications

2.1. Example 1: Thin film and near surface applications – Pendeo–epitaxial GaN defects

Although one of the great advantages of X-ray microdiffraction is the ability to probe beneath the surface of the sample, in many cases the ability to study the near-surface region is sufficient. Thin films are particularly appealing, as the phase sequence is known from the deposition pattern; key scientific questions can be addressed without the additional complication of differential aperture microscopy. A good example is a series of studies [10] of the defect distribution in GaN films grown by pendeo–epitaxial methods [11,12]. In these materials, electro-optically important GaN films are grown on patterned substrates (Fig. 4) with a goal of reducing the dislocations.

In the pendeo–epitaxial process, a homo-epitaxial single crystal surface layer is grown from seed layers previously grown on a single-crystal substrate and then patterned as illustrated in Figure 4. The technique is designed to reduce strains imposed by crystal-lattice mismatch and due to thermal expansion differences; a significant fraction of the growth is in wings which are not constrained as they extend over free space. In this example, the GaN stripes having a rectangular cross section and oriented along $[1\bar{1}00]$ were etched from 1 μm thick GaN single crystal layers grown by metal organic vapor phase epitaxy on 0.1 μm thick AlN buffer layer deposited on 6H–SiC (0001) substrate. After etching, GaN was grown and the subsequent overgrowth process was stopped after the wings from adjacent pedestals coalesced.

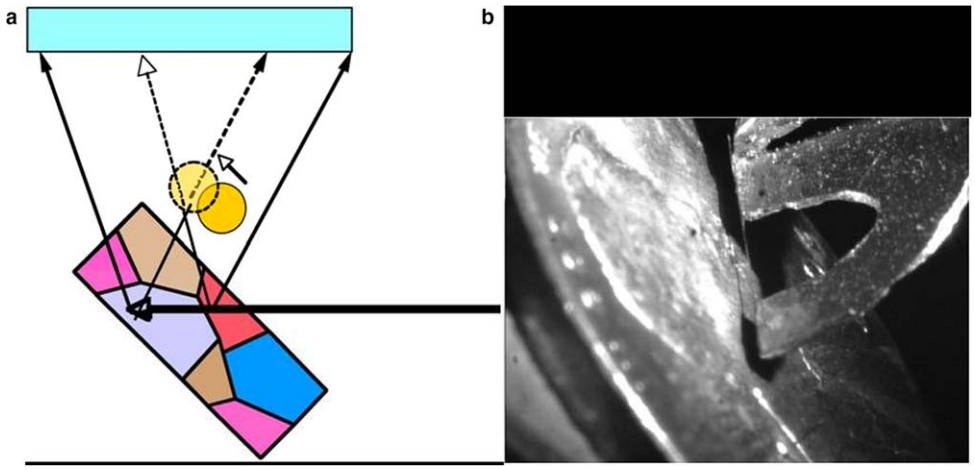

Figure 2. (a) Schematic of differential aperture microscopy technique. The wire is typically only a few hundred microns from the sample surface whereas the detector is approximately 200 mm from the wire. The ratio of distances is therefore around 10^3 which allows for good spatial resolution even though the detector pixel size is about 25 μm. (b) Actual wire shown near penny.

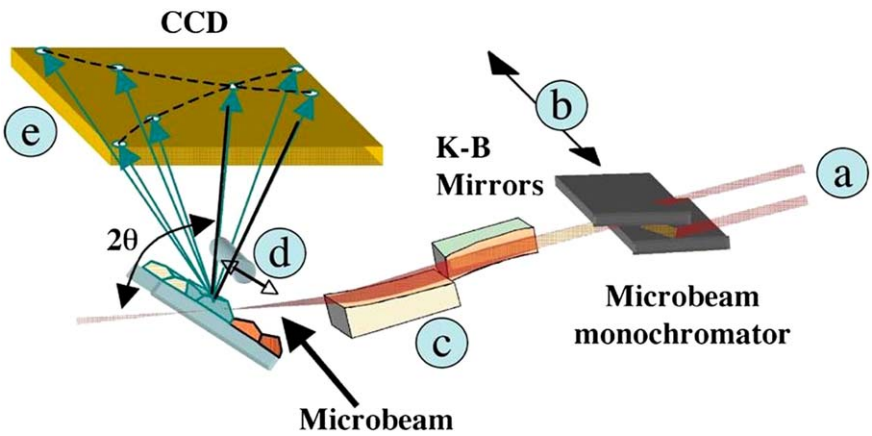

Figure 3. Key elements of the 3D X-ray crystal microscope. (a) The X-ray source is an intense synchrotron beam. (b) A special small-displacement microbeam monochromator can be inserted into or removed from the beam. (c) Nondispersive total-external reflection Kirkpatrick–Baez mirrors focus the beam to a submicron spot. (d) A smooth high-Z wire serves as the differential aperture to deconvolute the Laue patterns from along the incident beam. (e) A charge-coupled device with good spatial accuracy, low point-spread function, large dynamic range, low noise and fast readout is desirable.

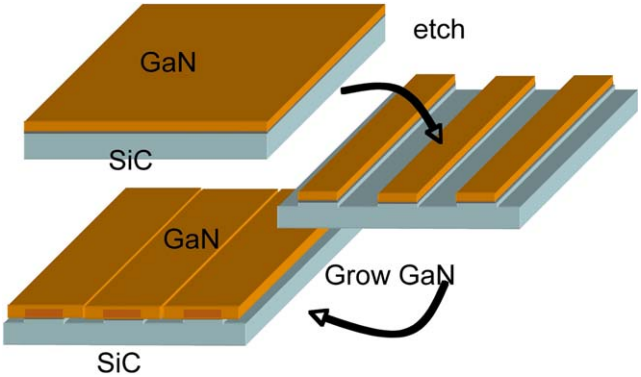

Figure 4. Schematic showing pendeo–epitaxial growth. A 1 μm GaN layer is grown from a single crystal of SiC on a 0.1 μm thick AlN buffer layer. The multilayer structure is then etched to create pedestals of SiC, AlN and GaN. The GaN is then grown over the pedestals and creates wings that eventually coalesce to produce a single crystal of GaN.

The white microbeam was scanned perpendicular to the stripe axis with a spacing of 0.25 μm. Due to the small size of the microbeam (~0.5 μm), it was possible to obtain separate images from different locations on the column and the wings. Because the high-energy X-ray beam passes through the GaN and the AlN layers, the SiC substrate contributes to the observed Laue patterns (see Fig. 1(b)). A typical line scan moves the sample under the beam in the X-axis which exposes different parts of the column, wing and substrate structure. Two Laue spots belonging to the SiC and GaN wings are shown at Figure 5. The SiC reflections do not change position with sample translation (uniform substrate orientation) and are used as a reference to refine the position of the GaN $(01\bar{1}8)$ Laue reflection. When the probing spot is moved along the positive X-axis and first hits the right wing of a stripe, the GaN reflection appears at the left side of the SiC reflections, as shown in Figure 5(a). As the probe spot is moved across the coalescence interface, two GaN reflections

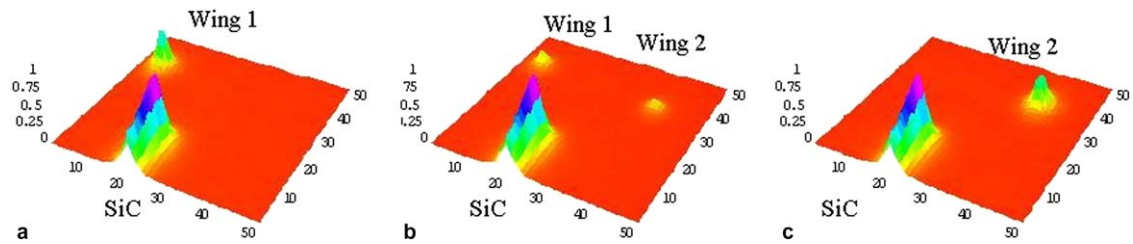

Figure 5. GaN and SiC Laue spots in the vicinity of the coalescence interface: (a) right wing of the stripe 1; (b) at the coalescence interface two wings from neighbor stripes give Laue spots symmetrically located relative to SiC spot; (c) left wing of the stripe 2.

can be observed simultaneously from both wings. They are located symmetrically relative to the SiC spot. With further displacement towards the left wing a second GaN stripe the GaN reflection from the left wing appears to the right of the SiC reflections (compare Figs. 5(a) and (c)). The shift of the GaN reflections along with the geometry of the GaN stripes structure, clearly indicates that at room temperatures the wings are tilted upward relative to the column in the coalesced GaN films.

2.2. Example 2: True 3D measurements – fractal deformation

The flow stress of metals deforming plastically by dislocation glide, is governed by dislocation–dislocation interactions. Recent acoustic emission measurements find that dislocation glide proceeds in a temporally intermittent manner. Temporal intermittency of plastic flow is associated with spatial heterogeneity and the formation of cellular dislocation patterns on various scales. Previous studies of dislocation patterning has found complicated patterning behavior that obeys power laws over a wide range of deformation. Other studies have demonstrated a fractal nature to the cellular dislocation structure and investigations of fractal patterning on the surface of deformed single metal crystals have shown spatial correlations from the nanoscopic to the microscopic scale [13].

Theoretical models to explain self-organized dislocation structure and slip bursts treats plastic deformation as an evolution of an extended dissipative dynamical non-equilibrium system. An important step to study the spatial correlations in plastic deformation is to monitor the plastic strain within the bulk, over various length scales from nanometers to millimeters. 3D X-ray microdiffraction is an ideal technique for this problem.

An experiment to study spatial correlations of plastic deformation monitored the 3D rotational behavior within a Cu single crystal. Measurements of the local lattice orientation were made as a function of depth and lateral position. A spatial resolution of 1 μm in the tensile direction and 1 μm in depth were achieved. Fractal behavior can be characterized by a Hurst exponent H. For this experiment, the Hurst exponent H measures the correlation of the misorientation of any element with the other elements in the data series as a function of distance L along the tensile length. The value of H was determined from the expression,

$$\langle \omega(G_x G_{x+L}) \rangle \propto L^H,$$

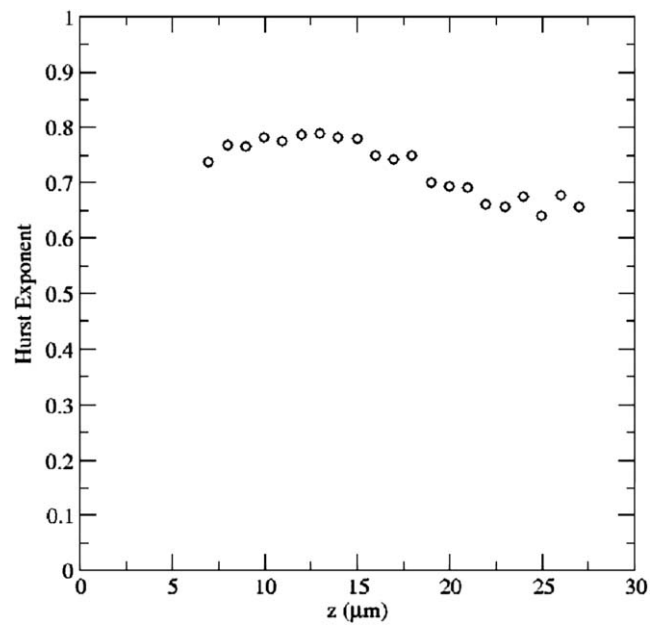

Figure 6. Hurst exponent for the rotational behavior of a 10% deformed Cu sample as a function of depth z beneath the sample surface.

where ω is the misorientation between the orientation tensor of positions x and $x + L$. And the expression $\langle \omega(G_x\ G_{x+L}) \rangle$ is the average of all the misorientations over all pairs of $(x, x + L)$.

A Hurst exponent of 0.5 indicates no long-term memory effect. Higher values indicate the data set is truly distinguishable from Gaussian or white noise [14,15]. The Hurst exponent H for the rotational behavior of the deformed Cu crystal is shown in Figure 6 as a function of depth z beneath the sample surface. A 3D self-affine rotational behavior was observed. It is noted that for as yet unknown reasons the fractal dimension drops gradually as depth increases.

3. Emerging areas

The main drawback of polychromatic microdiffraction with differential aperture microscopy is the time required to characterize sample volumes. Efforts are now underway to accelerate the data collection by the use of multiple wires (coded aperture) methods and by the use of

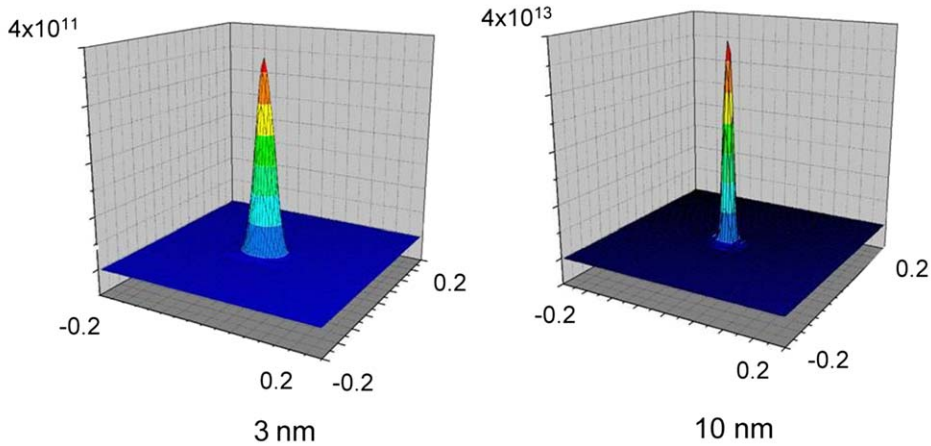

Figure 7. Even for very small particles on the order of 3–10 nm, Laue spots are sharp enough that the sample must be rotated to find a reflection. The left-hand graph shows the intensity distribution of a Laue spot at 90° to the incident beam from a spherical 3 nm face-centered cubic particle with a unit cell size of 0.35 nm. The units correspond to deviations $\Delta q/q$. The right-hand graph shows the intensity distribution of a Laue spot from a similar spherical 10 nm particle.

vastly faster detectors. These efforts are certain to have a major impact on the volume that can be probed and the statistical information that can be recovered; the scattering signal is sufficient to collect data in tens to hundreds of milliseconds, while the current detector readouts takes one to two orders of magnitude longer.

In addition, the use of scanning monochromatic methods opens the possibility of recovering not only full strain tensor information from sub-micron sample volumes, but also allows for unique measurements of diffuse scattering from samples – even weak diffuse scattering eight orders of magnitude weaker than Bragg scattering [7].

Polychromatic microdiffraction and related techniques are also essential for a wide range of experiments where high-spatial resolution is important or where samples cannot be rotated due to the presence of a complicated sample environment. For example, for spatially resolved measurements on samples less than 100 nm in size, sample rotations are difficult since it is hard to keep a small beam centered on such a small sample volume. Yet even for samples tens of nanometers in size, Bragg reflections are sharp and measurements with monochromatic beams require tedious sample rotations to determine structure (see Fig. 7).

With polychromatic microdiffraction however, the scattering intensity through a large volume of reciprocal space can be probed and 3D reciprocal space maps can be collected by scanning energy. Energy scans with non-dispersive monochromators avoid most of the problems associated with standard monochromatic measurements with signal-to-noise and reciprocal space resolution similar to standard monochromatic measurements.

Polychromatic microdiffraction is also emerging as an essential tool for studies where sample environmental chambers are difficult to orient. For example, polychromatic microdiffraction greatly simplifies measurements with high-pressure cells. Recent progress in this area indicates that polychromatic microdiffraction can help recover crystallographic information from small samples at very high pressures [16]. This is only the first example of experiments with novel sample environmental chambers that will benefit from polychromatic microdiffaction.

Acknowledgements

Work sponsored by the US Department of Energy, Division (DOE), Division of Materials Sciences and Engineering. Oak Ridge National Laboratory (ORNL) is operated by UT-Battelle, LLC, for the US Department of Energy under contract DE-AC05-00OR22725. Experiments were performed on Unicat beamline 34-ID at the Advanced Photon Source Argonne Il. Both 34-ID and the APS are supported by the DOE Office of Basic Energy Science.

The submitted manuscript has been authored by a contractor of the US Government under contract no. DE-AC05-00OR22725. Accordingly, the US Government retains a nonexclusive, royalty-free license to publish or reproduce the published or reproduce the published form of this contribution, or allow others to do so, for US Government purposes.

References

[1] H.F. Poulson, Philos. Mag. 83 (2003) 2761.
[2] H.F. Poulsen, S.F. Nielsen, E.M. Lauridsen, S. Schmidt, R.M. Suter, U. Lienert, L. Margulies, T. Lorentzen, D.J. Jensen, J. Appl. Cryst. 34 (2001) 751.
[3] W. Liu, G.E. Ice, J.Z. Tischler, A. Khounsary, C. Liu, L. Assoufid, A.T. Macrander, Rev. Sci. Instrum. 76 (2005) 113701.
[4] B.C. Larson, W. Yang, G.E. Ice, J.D. Budai, J.Z. Tischler, Nature 415 (2002) 887.
[5] J.S. Chung, G.E. Ice, J. Appl. Phys. 86 (1999) 5249.
[6] R.I. Barabash, G.E. Ice, B.C. Larson, G.M. Pharr, K.-S. Chung, W. Yang, Appl. Phys. Lett. 79 (2001) 749.
[7] G.E. Ice, R.I. Barabash, W. Liu, Z. Kristallogr. 220 (2005) 1077.
[8] R.I. Barabash, G.E. Ice, J.W.L. Pang, Mater. Sci. Eng. A 400–401 (2005) 125.

[9] G.E. Ice, B.C. Larson, W. Yang, J.D. Budai, J.Z. Tischler, J.W.L. Pang, R.I. Barabash, W. Liu, J. Synchrotron Rad. 12 (2005) 155.
[10] R.I. Barabash, G.E. Ice, W. Liu, S. Einfeldt, D. Hommel, R.M. Roskowski, R.F. Davis, Phys. Status Solidi A 5 (2005) 732.
[11] T.S. Zheleva, S.A. Smith, D.B. Thomson, T. Gehrke, K.J. Linthicu, P. Rajagopal, E. Carlson, W. Ashmawi, R.F. Davis, MRS Internet J. Nitride Semicond. Res. 4S1 (1999) G338.
[12] A.M. Roskowski, P.Q. Miraglia, E.A. Preble, S. Einfeldt, T. Stiles, R.F. Davis, J. Schuck, R. Grober, U. Schwarz, Phys. Stat. Sol. (a) 188 (2001) 729.
[13] M. Zaiser, F.M. Grasset, V. Koutsos, E.C. Aifantis, Phys. Rev. Lett. 93 (2004) 195507.
[14] J. Feders, Fractals, first ed., Plenum Press, New York, 1988, p283.
[15] B.B. Mandelbrot, J. Stat. Phys. 34 (1984) 895.
[16] G.E. Ice, P. Dera, W. Liu, H.-K. Mao, J. Synchrotron. Rad. 12 (2005) 608.